Materials Characterization 123 (2017) 128–136

Contents lists available at ScienceDirect

Materials Characterization

journal homepage: www.elsevier.com/locate/matchar

Effect of austenite grain size on the bainitic ferrite morphology and grain refinement of a pipeline steel after continuous cooling

H. Zhao, B.P. Wynne, E.J. Palmiere *

Department of Materials Science and Engineering, The University of Sheffield, Mappin Street, Sheffield S1 3JD, UK

ARTICLE INFO

Article history:
Received 3 August 2016
Received in revised form 16 November 2016
Accepted 17 November 2016
Available online 18 November 2016

Keywords:
Austenite grain size
Bainitic ferrite
Bain group
Close-packed plane group
Grain refinement

ABSTRACT

The effect of prior-austenite grain size (PAGS) on bainitic ferrite (BF) morphology and effective grain size in a pipeline steel under an industrial cooling condition was investigated. With PAGSs of 22.3 μm and 37.0 μm, BF laths with a parallel morphology could be seen, while as the PAGS is increased to 52.4 μm or 62.8 μm, more interlocking BF microstructures were observed. Detailed crystallographic analysis identified that intense BF variant selection occurs for the small-grained austenite, but due to the large austenite grain quantity, and thus the large total austenite grain boundary area per unit volume of the small-grained austenite, with the reduction of PAGS from 62.8 μm to 22.3 μm, the effective grain size of the transformed microstructure gradually decreases from 9.5 μm to 5.6 μm. The small-grained austenite transformation was dominated by one close-packed plane (CP) group, but for the larger austenite grain, different CP groups were observed to be adjacent to each other, producing the interlocking structure. A mechanism based on the carbon distribution near the BF/austenite interface is proposed to account for this difference.

1. Introduction

Bainitic microstructures have been widely used for enhancing mechanical properties of pipeline steels [1]. Owing to the low carbon concentration in these steels, cementite is usually absent, yielding a non-lamellar microstructure consisting of bainitic ferrite (BF) and micro-constituents such as martensite and retained austenite (M/A). The BF grows in the form of clusters of thin lenticular plates or laths, known as packets, and the formation of M/A constituents can be attributed to the partitioning of carbon from these BF laths to the austenite during cooling [2].

The importance of the prior-austenite grain size (PAGS) for bainite transformation is well acknowledged. Many investigations [3–6] have found that the rate of the bainite transformation is increased by decreasing PAGS, which was attributed to an increased austenite grain boundary density, and thus an enhanced nucleation rate. Conversely, other research has shown no appreciable effect of PAGS [7], or a reduction in the transformation rate with a smaller PAGS [8,9]. Additionally, the influence of PAGS has been suggested not to be continuous, and that there is a critical austenite grain size below which there is a distinct grain size effect [9]. To explain these conflicting observations, Matsuzaki and Bhadeshia [10] identified that different steels can show opposite PAGS effects, and that the discrepancy in kinetic behaviour is accompanied by obvious distinctions between the bainite microstructures. They hypothesised that the overall kinetics of the bainitic transformation is increased by a decrease in PAGS when the overall kinetics is limited by a slow growth rate, whereas the prior-austenite grain refinement reduces the overall kinetics for rapid growth from a limited number of nucleation sites. Furthermore, reducing PAGS has also been shown to lower the bainite-start temperature [5,11], and a new empirical equation for the bainite-start temperature, considering the effect of both chemical composition and PAGS has recently been developed [11].

Despite the number of studies concerning the effect of PAGS on BF transformation kinetics, there are few investigations regarding the influence of PAGS on BF microstructures and grain refinement. Therefore, in this research, specimens with various austenite grain sizes were processed in order to investigate the effect of PAGS prior to continuous cooling on the microstructural evolution and grain refinement.

2. Experimental Details

The chemical composition of the tested steel is shown in Table 1. The carbon content of this steel was lowered to 0.045 wt% to improve the weldability, toughness and the solubility of such high concentrations of niobium [12]. Titanium was added to fix nitrogen and refine the austenite grain during solidification and subsequent reheating.

In order to fully exploit the Nb concentration in this steel, and to fully dissolve its precipitates and shorten the preheating time during testing, all specimens were subjected to solid-solution heat treatments at 1250 °C using argon atmosphere protection, and were then water quenched directly from 1250 °C to room temperature.

* Corresponding author.
E-mail address: e.j.palmiere@sheffield.ac.uk (E.J. Palmiere).

http://dx.doi.org/10.1016/j.matchar.2016.11.025
1044-5803/

Table 1
Chemical compositions (wt%).

C	Mn	Si	S	P	Nb	Cr	Ni	Cu	Ti	N
0.045	1.43	0.14	<0.003	<0.01	0.09	0.21	0.12	0.21	0.01	0.0039

The processing route is schematically illustrated in Fig. 1. The heat treated specimens were reheated to 1200 °C at a rate of 10 °C/s, held for 2 min for equilibration, and then cooled at a rate of 5 °C/s to 1100 °C for a roughing deformation (strain1) at a constant true strain rate of 10 s^{-1}. Following roughing, the specimens were cooled immediately to 950 °C at a rate of 5 °C/s, followed by an accelerated cooling from 950 °C to 500 °C at a rate of 10 °C/s. After that, specimens were slowly cooled from 500 °C to 350 °C at a rate of 1 °C/s and finally water quenched from 350 °C to room temperature.

During the solid-solution heat treatment and the thermomechanical processing illustrated above, the parameters of the solid-solution heat treatment, the reheating and the roughing deformation (strain1) can influence the PAGS before the continuous cooling. However, attention must be given to choosing suitable parameters to generate different PAGSs, especially the reheating temperature and duration. During reheating, not only the PAGS, but also the dissolution status of the Nb precipitates are changed by altering the reheating temperatures or durations [13], which makes the investigation on the effect of PAGS biased. Provided that the standard solid-solution heat treatment can dissolve most of the Nb precipitates, then prolonging the duration of the heat treatment can result in a larger PAGS without greatly changing the Nb precipitate dissolution status. Additionally, changing the rough deformation (strain1) also has little influence on the Nb precipitate dissolution status simply due to the high temperature (1100 °C) of this deformation at which the solute supersaturation, and subsequently the extent of precipitation of Nb carbide or carbonitride is very small. Therefore, to generate austenite with different grain sizes, different parameters of the solid solution heat treatment and the rough deformation (strain 1) were used as shown in Table 2 and S, M, L and XL were designated to the specimens subjected to these different combinations of heat treatment durations and volumes of strain1. Additionally, specimen S, M, L and XL were also water quenched directly from 950 °C before the continuous cooling to reveal the prior-austenite microstructures exhibiting different PAGSs.

Samples for metallographic observation were cut in the rolling direction (RD) – normal direction (ND) plane and prepared carefully following standard methods [14]. A 2% nital solution was used to characterise the transformed microstructure, and a saturated aqueous picric acid solution was used to reveal the prior-austenite grain boundaries (PAGBs) [15,16]. PAGSs were measured optically using the linear intercept method.

EBSD analyses were also carried out *via* a FEI Sirion electron microscope with an HKL Nordlys detector. EBSD mappings with a step size of 0.2 μm and accelerating voltage of 20 kV, and were performed on the RD-ND plane of each sample.

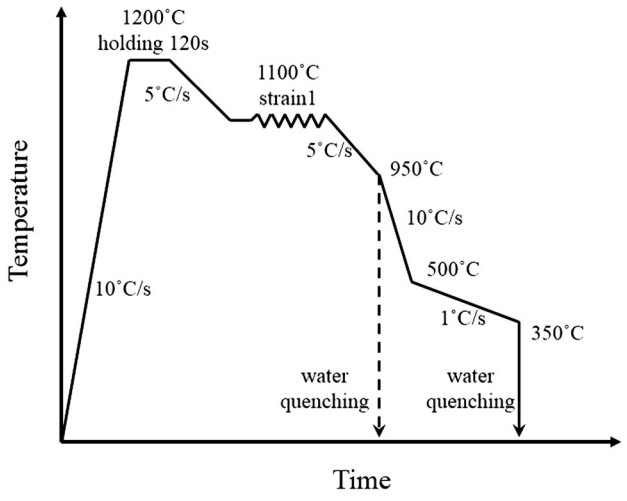

Fig. 1. Schematic illustration of the thermomechanical testing profile.

Table 2
Heat treatment and austenite deformation parameters.

Specimen names	S	M	L	XL
Heat treatment temperature (°C)	1250	1250	1250	1250
Heat treatment duration (s)	1800	1800	7200	7200
Strain1 volume	0.7	0.3	0.3	0
Prior-austenite grain size (μm)	22.3	37.0	52.4	62.8

3. Results

3.1. Prior-austenite Microstructures

Optical micrographs of the prior-austenite grain boundaries (PAGBs) before the continuous cooling for specimen S, M, L and XL are shown in Fig. 2. It is clear from Fig. 2(a) –(d) that through adjusting the solid-solution heat treatment durations and the volumes of strain1, fully recrystallised austenite with different grain sizes were successfully developed before the continuous cooling. PAGS measurement results are shown in Table 2, showing PAGS varying from 22.3 μm to 62.8 μm.

3.2. Transformed Microstructures

Optical micrographs of the continuously cooled microstructures with different PAGSs are shown in Fig. 3. The transformed microstructures all consist of BF but with clear differences in their morphologies. With PAGS of 37.0 μm, Fig. 3(b), the transformed microstructure mainly consists of packets of parallel BF laths. With an increased PAGS, Fig. 3(c)–(d), the BF lath boundaries are more and more obscure and irregularly shaped, and the shape of the M/A constituents also changes from acicular to equiaxed. Due to the very small PAGS (22.3 μm), the microstructure shown in Fig. 3(a) is well refined, and the morphology of the BF microstructure cannot be observed clearly from this optical micrograph.

To observe the transformed microstructures in greater detail, SEM secondary electron micrographs of the continuously cooled microstructures with different PAGSs are shown in Fig. 4. With PAGSs of 22.3 μm and 37.0 μm, BF laths with a parallel morphology can be clearly observed. However, as the PAGS is increased to 52.4 μm or 62.8 μm, more interlocking BF microstructures are observed in Fig. 4(c)– (d). In these microstructures, BF laths with different directions intersect with each other.

3.3. EBSD Mappings

A small area of each EBSD mapping data set was used to plot an inverse pole figure (IPF) coloured orientation map and a corresponding boundary map. For a statistical analysis of the boundary interception length and boundary density distribution, each whole data set was used.

The selected area IPF coloured orientation maps and corresponding boundary maps of the continuously cooled microstructures with different PAGSs are shown in Fig. 5. It can be seen from Fig. 5 that with an increasing PAGS, the density of high angle grain boundary (HAGB, $\theta \geq 15°$) is reduced and the fraction of low angle grain boundary (LAGB, $15° > \theta > 3°$) is increased, where θ is the boundary disorientation angle. More importantly, as the PAGS is increased, the shape of the LAGB changes from being effectively parallel and straight to being